This is a peer-reviewed, accepted author manuscript of the following research article: Ye, J., Quan, G., Kyvelou, P., Teh, L., & Gardner, L. (2022). A practical numerical model for thin-walled steel connections and built-up members. *Structures*, *38*, 753-764. https://doi.org/10.1016/j.istruc.2022.02.028

A practical numerical model for thin-walled steel connections and built-up members

Jun Ye[1], Guan Quan[2], Pinelopi Kyvelou[1], Lip Teh[3], Leroy Gardner[1]

[1] Department of Civil & Environmental Engineering, Imperial College London, London SW7 2AZ, UK

[2] College of Civil Engineering and Architecture, Zhejiang University, Hangzhou, 310058, China

[3] School of Civil, Mining & Environmental Engineering, University of Wollongong, Wollongong, NSW 2522, Australia

Abstract: The interaction between the cold-formed steel members and fasteners in a structural assembly often involves complex stress states, material plasticity, significant in-plane deformations and curling, rendering computational modelling of the resulting structural system challenging. In addition, the presence of initial geometric imperfections and the susceptibility of cold-formed steel members to local instabilities adds a further degree of complexity to the numerical modelling. The behaviour of bolted connections between cold-formed steel members has traditionally been assessed based on physical tests, though these can be time consuming and expensive. In this paper, a practical numerical approach to the simulation of bolted cold-formed steel connections, capturing all the key behavioural features including bolt preload, slippage and bearing, is introduced. Starting from a typical shell finite element (FE) model of a cold-formed steel plate, a small number of solid elements is introduced around the bolt holes, to allow accurate replication of the bolt-ply interaction, with contact pairs defined between the bolts and the surrounding material. An explicit dynamic solver is then employed to solve the geometrically and materially nonlinear problem, both with and without bolt slippage. Validation of the FE model is conducted using benchmark tests reported in the literature. It is shown that the proposed numerical method can accurately capture the structural behaviour of bolted cold-formed steel connections and cold-formed steel built-up sections, while being computationally efficient and numerically stable; the proposed approach is therefore recommended for the numerical modelling of cold-formed steel systems assembled using fasteners.

Keywords: bolted connections, built-up sections, cold-formed steel, computational modelling, fasteners

1 Introduction

Various codes of practice [1-3] have been developed for the design of cold-formed steel structures, covering their wide range of applications spanning from conventional secondary to primary frame members, and, more recently, to modular construction and long-span members using built-up cross-sections. Connections are an important feature of such structures since their response can have a crucial impact on the structural behaviour of the connected members and, ultimately, of the overall system.

There are numerous types of connectors used in cold-formed steel construction, employed either between cold-formed steel members or between cold-formed steel and hot-rolled steel, timber or concrete members. The most commonly employed types of steel-to-steel connections are shown in Fig. 1, featuring bolts, screw fasteners, spot welds, blind rivets, power actuated fasteners and clinching connections; bolts are particularly widely used, with the bolt holes usually being punched during the section forming process.

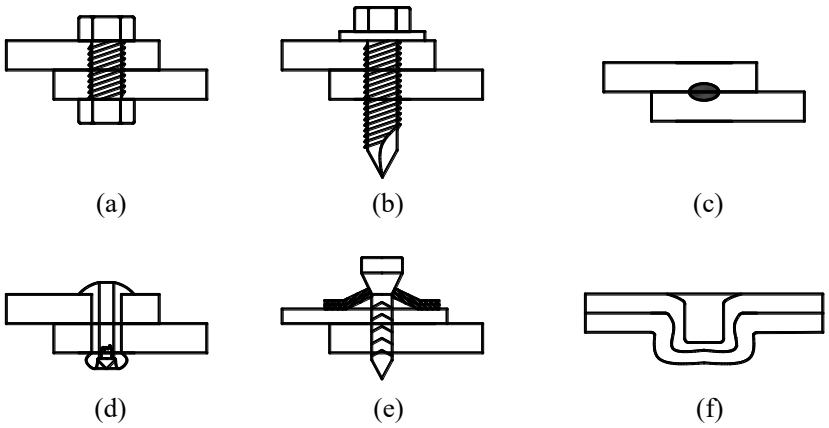

Fig. 1 Fastener types used in cold-formed steel construction: (a) bolts (b) self-tapping screws (c) spot welds (d) blind rivets (e) power actuated fasteners (cartridge fired pins) (f) clinching connections

Early research by Winter [4] on cold-formed steel bolted connections led to the recognition and definition of four distinct failure modes, namely block shear failure, tear-out (or shear-out) failure, bearing failure and net section failure [5-9]; the latter three types of failure are shown in Fig. 2. In [4] and [10], the influence of bolt slippage and initial tightening torque in bolted cold-formed structural systems was also demonstrated. This early work, in combination with Winter's later research [11], served as the basis for the design equations that appear in a number of international codes of practice [1-3], with some revisions [8, 12] and design equations for the block shear failure mode [5] having been incorporated in the more recent versions of these codes.

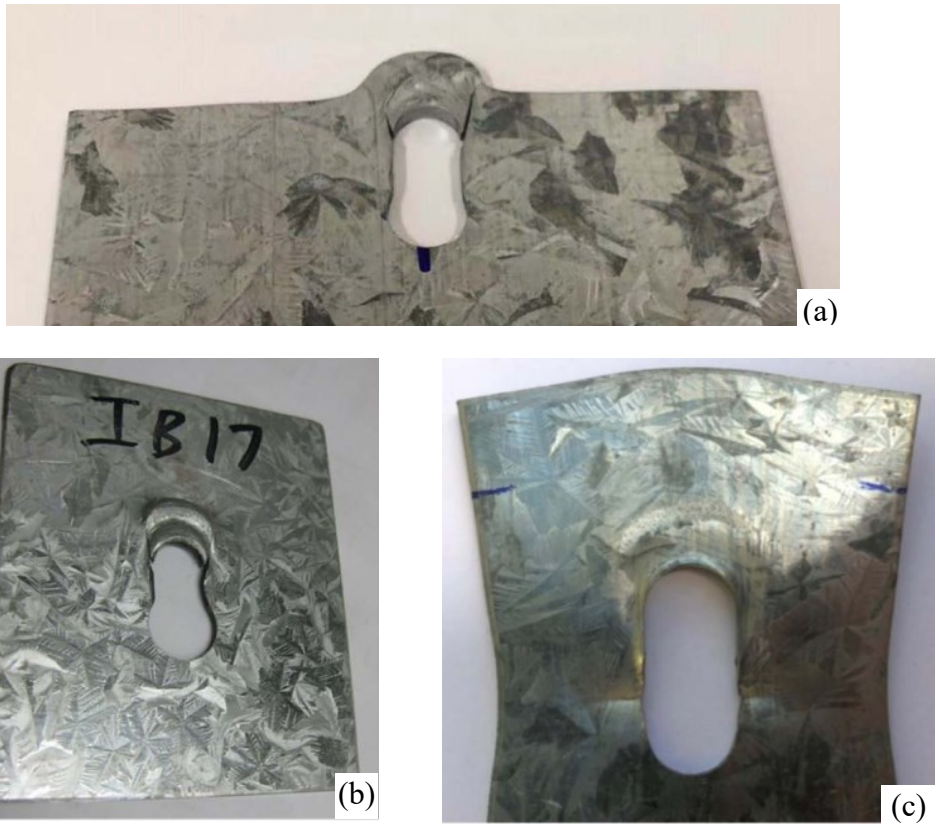

Fig. 2 Typical failure modes of bolted connections: (a) shear-out failure; (b) bearing failure; (c) net section failure [9]

Bolted connections between thick hot-rolled steel and stainless steel plates have been extensively investigated through experimental and numerical research, both for normal and high-strength materials [13-19]. While the design equations for bolted connections have been traditionally developed through experimental testing and analysis, in recent years, numerical modelling has been employed to complement experimental results [15-20]. However, recent research on the numerical modelling of hot-rolled steel bolted connections has shown that there can be substantial differences between the stiffness values determined from physical testing and those predicted by finite element (FE) modelling [20]. Such discrepancies are even more prominent for thin-walled cold-formed steel connections, where the well-established modelling techniques for conventional hot-rolled steel structures may not be directly applicable. This is attributed to influence of the ratio of the bolt diameter to the thickness of the connected plate: for typical bolted connections in hot-rolled steel, the bolt diameter and thickness are roughly the same, but in the case of cold-formed steel, the bolt diameter is generally substantially greater than the plate thickness. In the latter case, penetration of the bolt threads into the thin-walled steel ply and the subsequent bulging effect, shown in Fig. 3, which is restrained by the bolt head and nut, can have a significant influence on the behaviour of the connection, complicating the FE simulation.

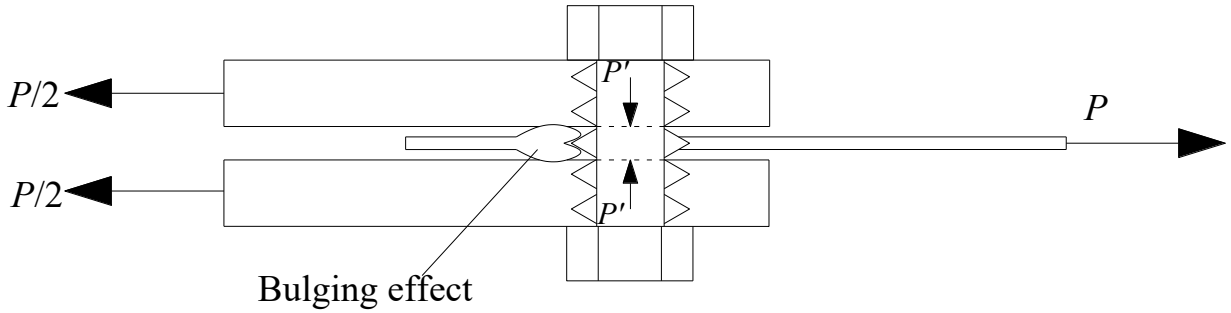

Fig. 3 Thread penetration and bulging effect in thin steel plate, leading to the development of tensile force P' in the bolts

The conventional approach to modelling bolted connections in cold-formed steel is to use solid elements, such as C3D8R in ABAQUS, to discretise the plates [21-24]. However, the modelling of connections that include a number of bolts, as is typically the case in cold-formed steel, is both technically and computationally challenging. The study presented herein aims to develop a numerical methodology that can realistically and efficiently replicate the behaviour of bolted connections between cold-formed steel members subjected to monotonic loading. Starting from a shell-based FE model, a small number of solid elements are employed around the bolt holes, to allow for an accurate definition of the contact interaction between the bolts and the surrounding plies. Preloading of the bolts is applied using a temperature field and a dynamic solver is utilised for the FE analysis, incorporating geometric and material nonlinearities and accounting for bolt slippage. Comparisons with physical tests reported in the literature are used to demonstrate the effectiveness of the proposed numerical methodology.

2 Conventional modelling techniques

Finite element analysis (FEA) has been widely used in the past to study the nonlinear behaviour of thin-walled structural assemblies, such as stud walls, connections and built-up sections [25, 26]. In such assemblies, cold-formed steel members are part of a complex structural system in which the interaction between the various components needs to be accounted for in order to realistically replicate the overall structural behaviour [25]. Simulation of the connections between the system components is therefore crucial.

A number of techniques has been used to date for the modelling of bolted connections in cold-formed steel. Modelling is often proceeded by physical testing to ascertain the bearing force-deformation relationship that can be incorporated into the model. Lim and Nethercot [27] developed a numerical model to study the structural behaviour of cold-formed steel portal frame systems, comprising cold-formed steel members connected back-to-back with bolts and bracket plates. The cold-formed steel members were modelled using shell elements, while the bolts were replicated by nonlinear spring elements that were assigned force-elongation relationships determined from previously conducted double-shear lap tests – see Fig. 4(a). A schematic illustration of the employed nonlinear springs is shown in Fig. 4(b). This method of modelling bolted connections between cold-formed steel members has been also adopted by other researchers [28, 29], with reasonable agreement achieved between the test and FE results. A similar approach has been followed in [30], where a user-defined element was assigned a load-deflection curve determined from shear tests on screw fasteners, to model the behaviour of cold-formed steel built-up columns. However, this method is reliant on the accuracy and limited by the scope of the underpinning test data; it can also result in significant membrane deformations developing at the ends of the nonlinear springs, leading to a local underestimation of the stiffness – see Fig. 4(c).

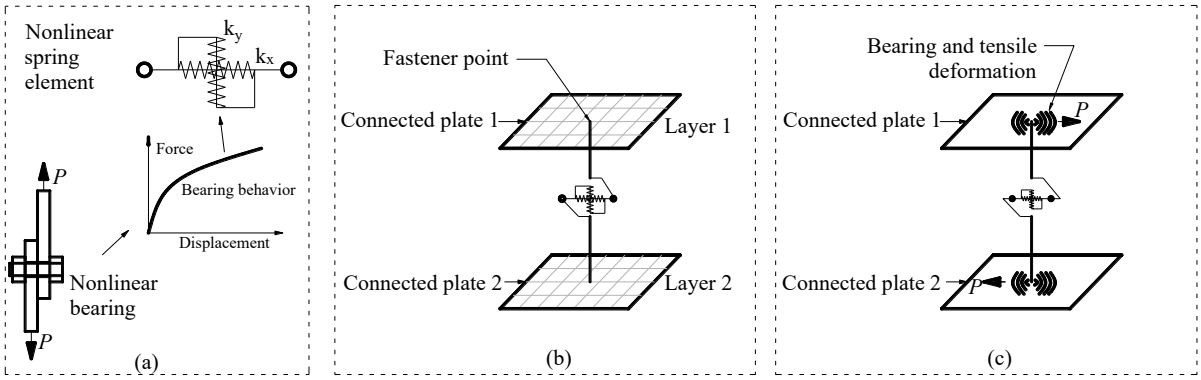

Fig. 4 Modelling of bolted connections using nonlinear springs [27]

Rinchen and Rasmussen [31] determined the load-displacement responses of a series of bolted and screwed connections experimentally, which were subsequently incorporated into numerical simulations through nonlinear springs to examine the structural behaviour of cold-formed steel portal frames. In order to reduce the membrane deformation developed at the two ends of the nonlinear spring elements, a "connector element", with the physical radius of the fastener, was introduced, as shown in Fig. 5, with all the nodes located on the physical radius being kinematically coupled with the end points of the connector element. This technique was found to reduce the stress and strain concentration at the connector ends significantly, and to yield more accurate stiffness predictions. It is worth noting that in the connector element, as shown in Fig. 5(a), bolt slippage can also be accounted for by introducing a plateau in the bearing force-deformation response assigned to the springs.

More recently, Kechidi *et al*. [30] developed a user-defined element including load-deflection curves of a series of screw fasteners, determined from tests, to model the behaviour of cold-formed steel built-up columns, while Ye *et al*. [32-35] successfully replicated the behaviour of built-up beams and bolted connections subjected to monotonic and cyclic loading. Phan and Rasmussen [36] numerically simulated cold-formed steel built-up sections subjected to bending about their minor axis, where the connectors were modelled as nonlinear springs which were assigned force-bearing deformation relationships obtained from single shear tests on bolted joints.

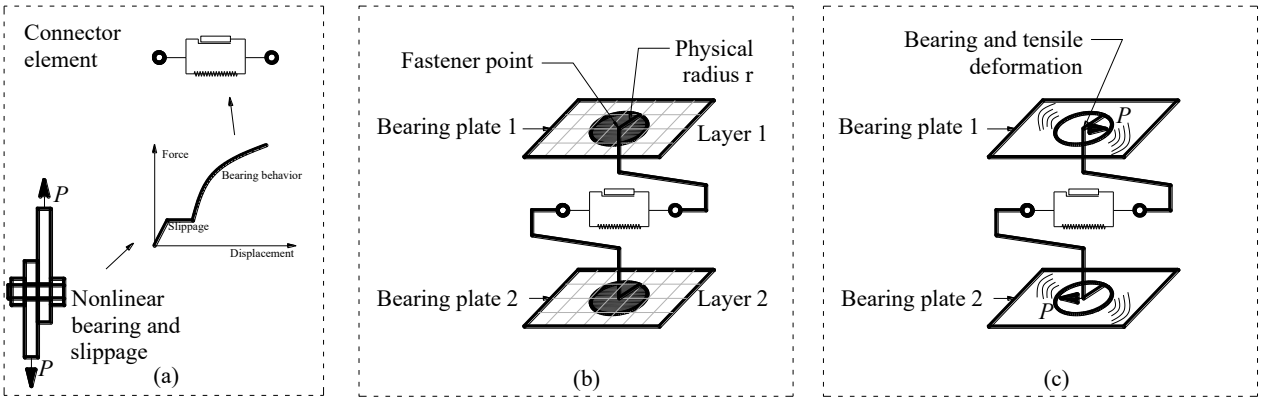

Fig. 5 Use of nonlinear connectors in the modelling of fasteners in bolted connections

Chung and Ip [37] successfully developed nonlinear FE models using three-dimensional solid elements to investigate the structural performance of bolted connections between cold-formed steel strips in shear. The results were accurate, but the exclusive use of solid elements for the modelling of structural systems comprising a number of cold-formed steel members and fasteners can lead to excessive computational cost. In contrast, shell elements can accurately replicate the response of cold-formed steel structural elements, while remaining relatively computationally efficient [38]. The combined use of solid and shell elements is advocated in the present study, as detailed in the following section.

3 Key features of developed numerical model

In this section, a novel modelling technique is proposed to simulate the response of cold-formed steel members with bolted connections. Seeking to combine computational efficiency and accurate replication of localised physical phenomena, FE models comprising shell elements and a small number of solid elements around the bolt holes are developed in ABAQUS [39], accounting for both geometric and material nonlinearities. The key features of the developed FE models are presented in this section.

3.1 Material model

The Ramberg-Osgood model [40], given by Eq. (1), which is frequently employed to describe the rounded stress-strain behaviour of metals, is adopted herein for modelling the material response of the examined cold-formed steel connections. In Eq. (1), σ and ε are the engineering stress and strain respectively, E is the Young's modulus, f_y is the yield (0.2% proof) stress, f_u is the tensile strength, ε_u is the strain at f_u and n, defined by Eq. (2), is the strain hardening exponent defining the degree of roundness of the stress-strain curve. Predictive models for the key input parameters of the single, and the more accurate two-stage Ramberg-Osgood expressions, for cold-formed steel are presented in [41]:

$$\varepsilon = \frac{\sigma}{E} + 0.002\left(\frac{\sigma}{f_y}\right)^n \tag{1}$$

$$n = \frac{\ln(\varepsilon_{us}/0.002)}{\ln\left(f_u/f_y\right)} \tag{2}$$

$$\varepsilon_{us} = \varepsilon_u - f_u/E \tag{3}$$

For input into ABAQUS [39], the engineering stresses and strains were transformed into true stresses σ_{true} and true plastic strains ε^{pl}_{true}, according to Eqs. (4) and (5).

$$\sigma_{true} = \sigma\,(1+\varepsilon) \tag{4}$$

$$\varepsilon^{pl}_{true} = \ln(1+\varepsilon) - \sigma_{true}/E \tag{5}$$

3.2 Elements and contact properties

Shell elements are typically preferred over continuum elements for the modelling of cold-formed steel structural members due to their high computational efficiency. However, solid elements can provide a more detailed and accurate replication of localised bearing phenomena. Therefore, for the FE model introduced herein and shown in Fig. 6, shell elements are employed for the modelling of the material away from the bolt holes, while solid elements are used for the modelling of the bolts and the cold-formed steel sheet around the bolt holes, in order to accurately capture the localised bearing of the bolts against the cold-formed steel. Rectangular openings are made in the shell element mesh around the bolt holes; the openings are then filled with solid elements using the *EXTRUDE command in ABAQUS [39]. Round bolt holes are finally modelled at the centre of the block comprising the solid elements. Special attention is given to ensure that the size of the block around the bolt hole meshed with solid elements is sufficiently large to cover the areas of major influence of the bolt nut and bolt head. A typical example of the proposed modelling method is shown in Fig. 6, while typical cross-sections of joints are presented in Fig. 7.

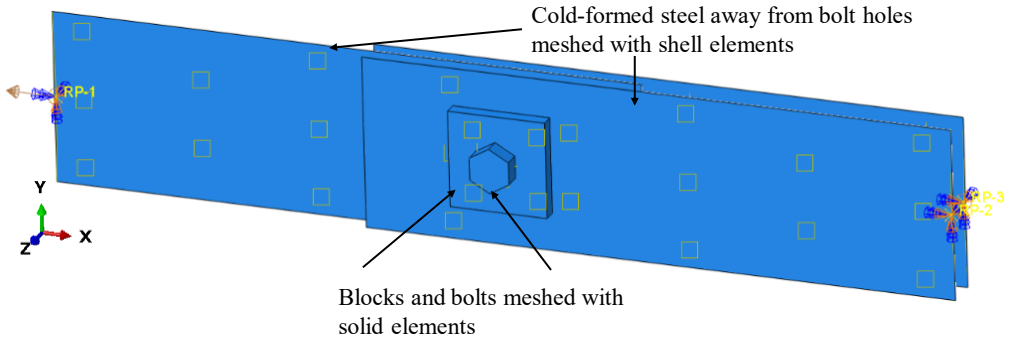

Fig. 6 Use of solid and shell elements in a typical model of a double-shear lap connection

The contact interactions between the bolt head/nut and the block, and between the inner and the outer plates are modelled using surface-to-surface contact with Coulomb friction in the tangential direction. A friction coefficient μ of 0.15 between the cold-formed steel sheets and bolts, recommended in [4], is employed for all the FE analyses conducted herein. The contact normal to the surface is defined as "hard" to prevent penetration of the surfaces into each other. Contact pairs are also created between the bolts and the plates using surface-to-surface contact properties for non-threaded bolts and general contact properties for threaded bolts – see Fig. 7. Finally, the slave surfaces are allowed to separate from their corresponding master surfaces, thus preventing tensile stresses from developing at their interface.

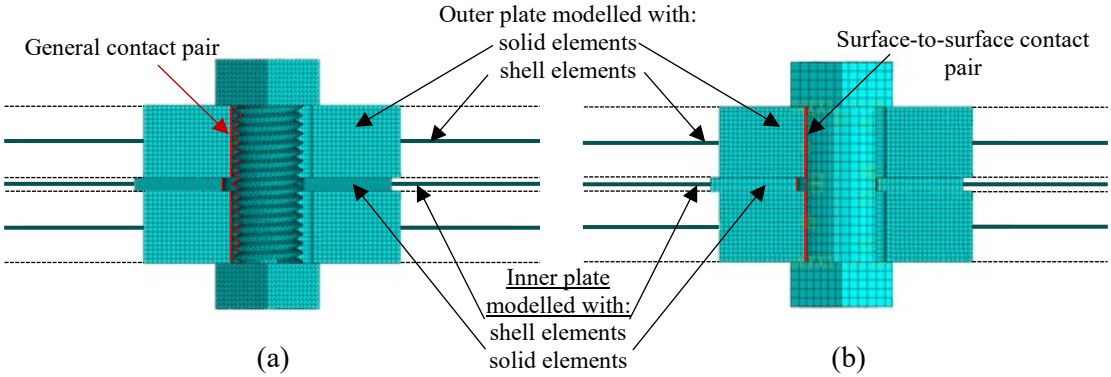

Fig. 7 Cross-section of joint with (a) threaded and (b) non-threaded bolt

3.3 Solver scheme

Static solvers, such as those employed in ABAQUS [39] often suffer numerical convergence difficulties [25] when applied to problems of the nature examined in this paper. In such cases, the use of an explicit dynamic solver is recommended. Explicit dynamic analyses are based on large-deformation theory, comprise a large number of successive time increments (which are relatively inexpensive computationally) and adopt an explicit central difference integration scheme, which requires a time increment limit to ascertain numerical stability. An estimation of the computational time increment limit is given by:

$$\Delta t_{\text{stable}} = L_{\text{e}} / c_{\text{d}} \tag{6}$$

where L_{e} is the minimum length of the adopted element faces and c_{d} is the wave velocity of the material, given by:

$$c_{\text{d}} = \sqrt{E / \rho} \tag{7}$$

where ρ is the density of the material.

With the computational time increment limit being dependent on the size of the elements, a careful balance is required to ensure that the mesh is fine enough to accurately replicate the exhibited structural response, yet coarse enough to achieve computational efficiency. Mass scaling [39] can also be used to improve computational efficiency further. However, special attention needs to be given to ensure that the adopted loading rate does not result in increased inertial forces that can alter significantly the solution. A simulation is considered to be quasi-static when the total kinetic energy of the model is negligible compared to its total internal energy (or when the reaction force in the time history is approximately equal to the applied action) [42, 43].

3.4 Bolt pretension and slippage

In cold-formed steel bolted connections, bolt pretension (applied in practice via the bolt head with a torque wrench), combined with the clearance of the bolt hole, typically result in slippage at a certain load level, which will be apparent in the load-extension curves [4]. The torque-preloading relationship is often described by means of a constant K, known as the torque coefficient, as shown in Eq. (6) [44, 45].

$$T = K P_{\text{b}} d \tag{8}$$

In Equation (8), T is the torque applied to the bolt head or nut, P_{b} is the preloading force and d is the nominal bolt diameter. For the FE analyses conducted herein, in line with [44, 45], a value of 0.2 has been assigned to the torque coefficient K. The bolt slip resistance for a given

applied torque can be then calculated according to Eq. (9) [46], where μ is the friction coefficient (taken as 0.15 [4]) and n_b is the number of slip surfaces.

$$F_{slip} = \mu P_b n_b \quad (9)$$

In ABAQUS [39], it is common practice to use the 'Bolt Load' command for the application of bolt pretension. However, since this command is not available when an explicit dynamic solver is used, a different method is followed herein. An initial step is first employed for the definition of the boundary conditions and contact pairs of the modelled connection, followed by a 'prestress step' using a dynamic explicit solver and, finally, a loading step using a dynamic solver for the application of the connection loads.

Two different methods have been examined for the implementation of the bolt pretension during the second step of the FE analysis: (i) definition of a decreased temperature field for the bolt shank resulting in the development of tensile forces (and thus pretension), and (ii) use of a 'Contact Interference Fit' analysis [39], where an initial overclosure is defined between the contact pairs, resulting in the development of internal pressure in the bolt shank. The first method was found to be more stable numerically while yielding accurate slippage predictions (as shown in Section 4.1); its use is therefore recommended and has been employed for all FE analyses presented herein.

4 Application and validation of proposed numerical method

The application and validation of the proposed numerical method is assessed in this section by comparisons against physical tests reported in the literature. Two different applications of this method are examined: (i) cold-formed steel lap connections and (ii) cold-formed steel built-up sections.

4.1 Cold-formed steel lap connections

The accuracy and stability of the proposed approach for the modelling of lap connections in cold-formed steel are assessed in this sub-section through comparisons with the results of physical tests. In [27] and [37], a series of experiments on bolted lap connections was undertaken to investigate the bearing behaviour of bolts against cold-formed steel plates. In [27], both fully-threaded and partially-threaded M18 bolts were employed, while in [37] the employed fasteners were partially-threaded M12 bolts. In the case of the partially-threaded bolts, the shear planes and bearing contact areas lay within the non-threaded shank region of the bolts. Both the fully-threaded and partially-threaded bolts were considered in the model validation presented herein. The nominal dimensions of the tested specimens are shown in Fig. 8. More details regarding the test setup and specimen characteristics can be found in [27] and [37].

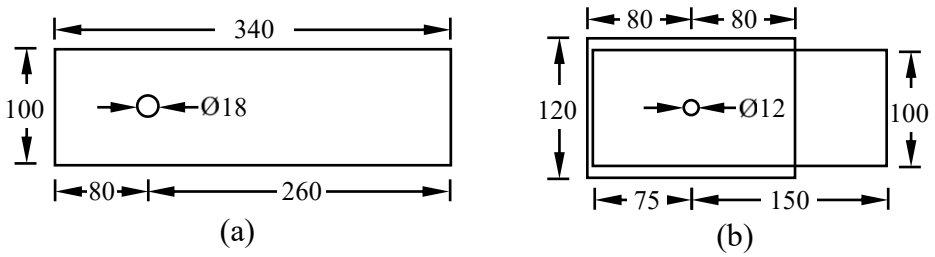

Fig. 8 Nominal dimensions (in mm) of specimens for lap tests reported in: (a) [27] and (b) [37]

The 4-noded quadrilateral S4R shell element with reduced integration [39] was employed for modelling the cold-formed steel plates away from the bolt holes while the hexahedral 8-noded brick element C3D8R with reduced integration [39] was used to model the bolt and the area of the plates around it. For the modelling of the threaded bolt, 4-noded linear tetrahedral C3D4 elements were also employed to capture the intricate geometry of the threads.

The mesh and boundary conditions of the developed FE models are presented in Fig. 9. To replicate the boundary conditions of the tested joints, all nodes on the edges of the hot-rolled and cold-formed steel plates were coupled to reference points which were constrained as shown in Fig. 9. For the conducted numerical analyses, the material properties assigned to the modelled specimens were obtained from material tests reported in [27] and [37].

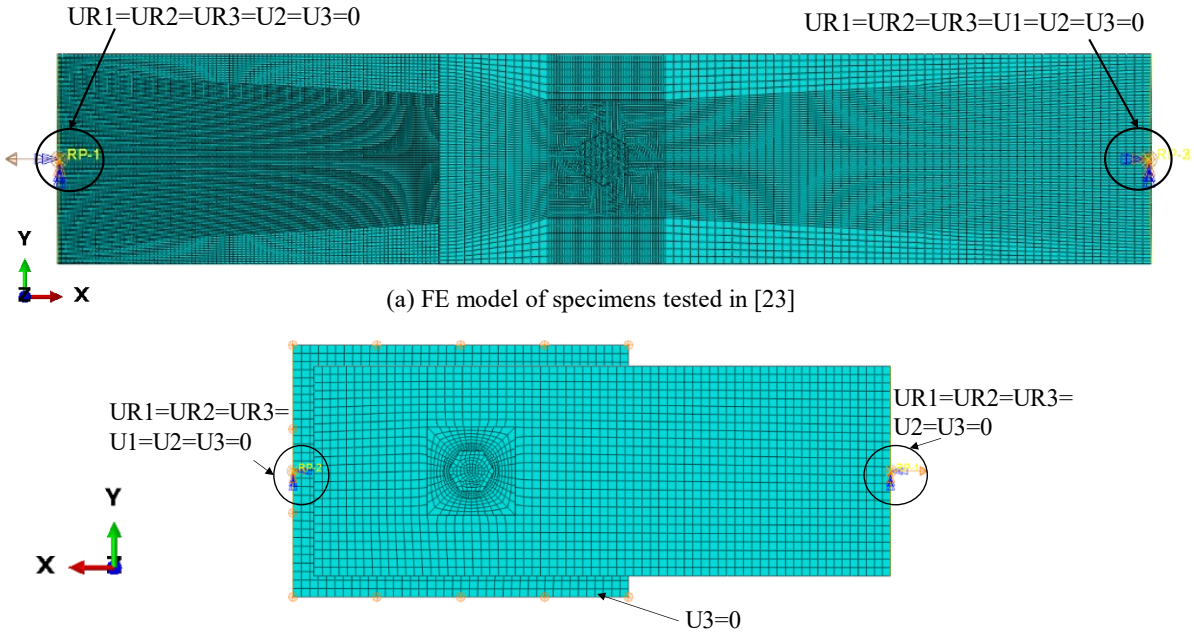

(a) FE model of specimens tested in [23]

(b) FE model of specimens tested in [33]

Fig. 9 Mesh and boundary conditions of FE models

As shown in Fig. 10, a total of 2400 s was used in the explicit FE analyses. As explained in Section 3.3, mass scaling [39] was employed, with the target time increment set to 0.02 s for the lap joints with the partially-threaded bolts. For the threaded bolt specimens, explicit modelling of the threads resulted in reduced element dimensions and, therefore, in a time increment of 0.01 s required to achieve computational efficiency.

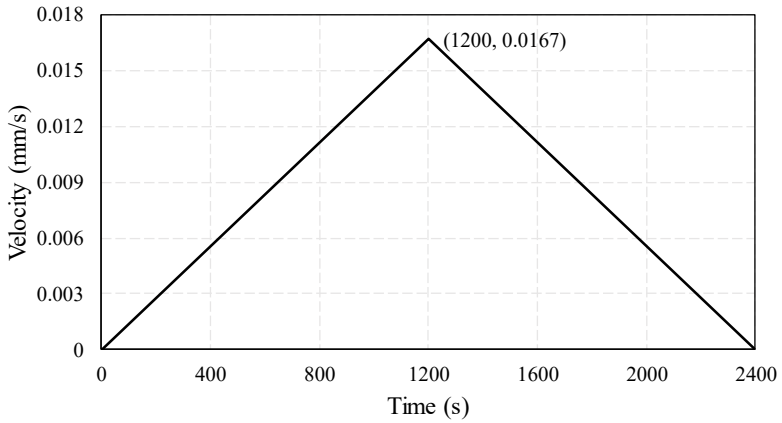

Fig. 10 Velocity-time relationship employed in explicit FE analyses of cold-formed steel lap connections

Comparisons between typical load-extension test and FE curves are shown in Fig. 11, where it can be observed that the FE models yield accurate predictions for both types of joint (i.e. with fully-threaded and partially-threaded bolts). The von Mises stress contours in the test plates at an extension of 3 mm are shown in Fig. 12, while the evolution of plasticity around the bolts is shown in Fig. 13, where it can be observed that, as expected, with increasing extension of the connection, the extent of yielding in the plates gradually increases. Note that failure of the lap joints presented in Fig. 11 involved fracture of the material, which is not considered in the proposed modelling approach; hence the peak and post-peak stages of the load-extension curves are not compared.

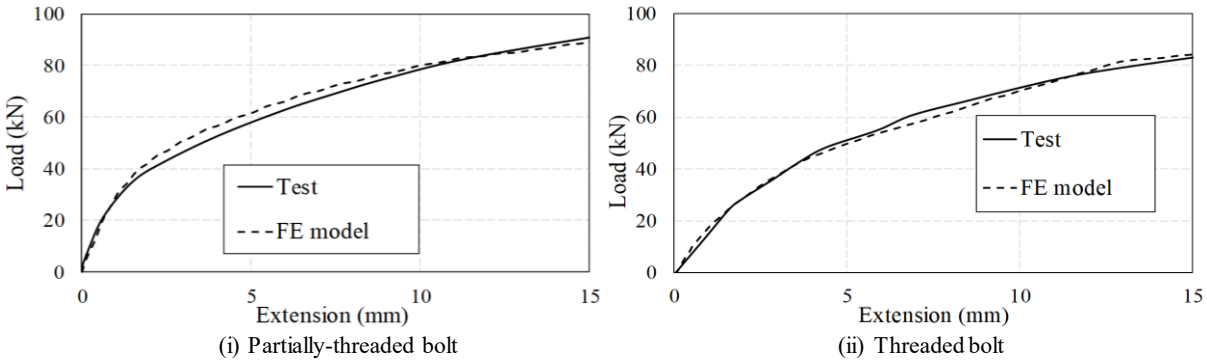

(a) Lap joints in [23]

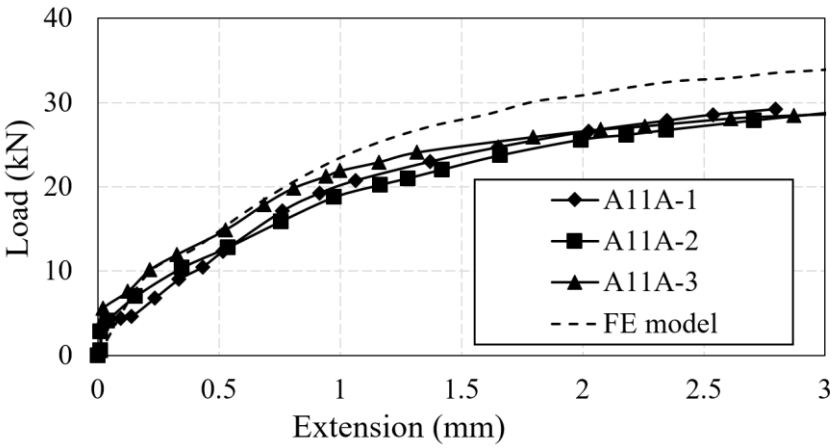

(b) Lap joints in [37]

Fig. 11 Comparisons between test and FE load-extension curves of lap joints

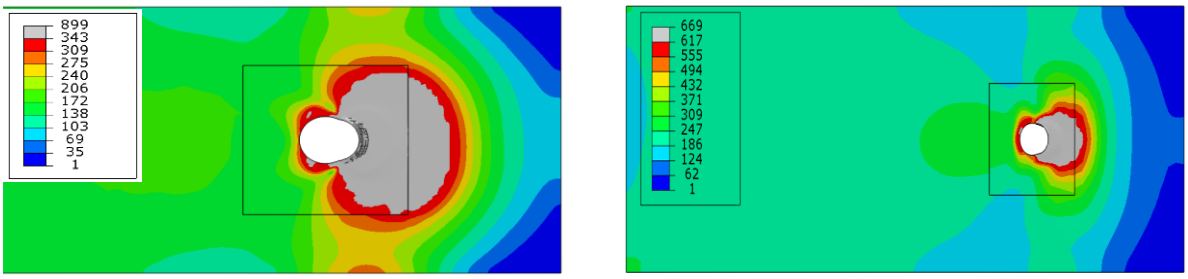

(a) (b)

Fig. 12 Von Mises stress contours at 3 mm extension of specimen tested in (a) [27] and (b) [37] (contour units: N/mm^2)

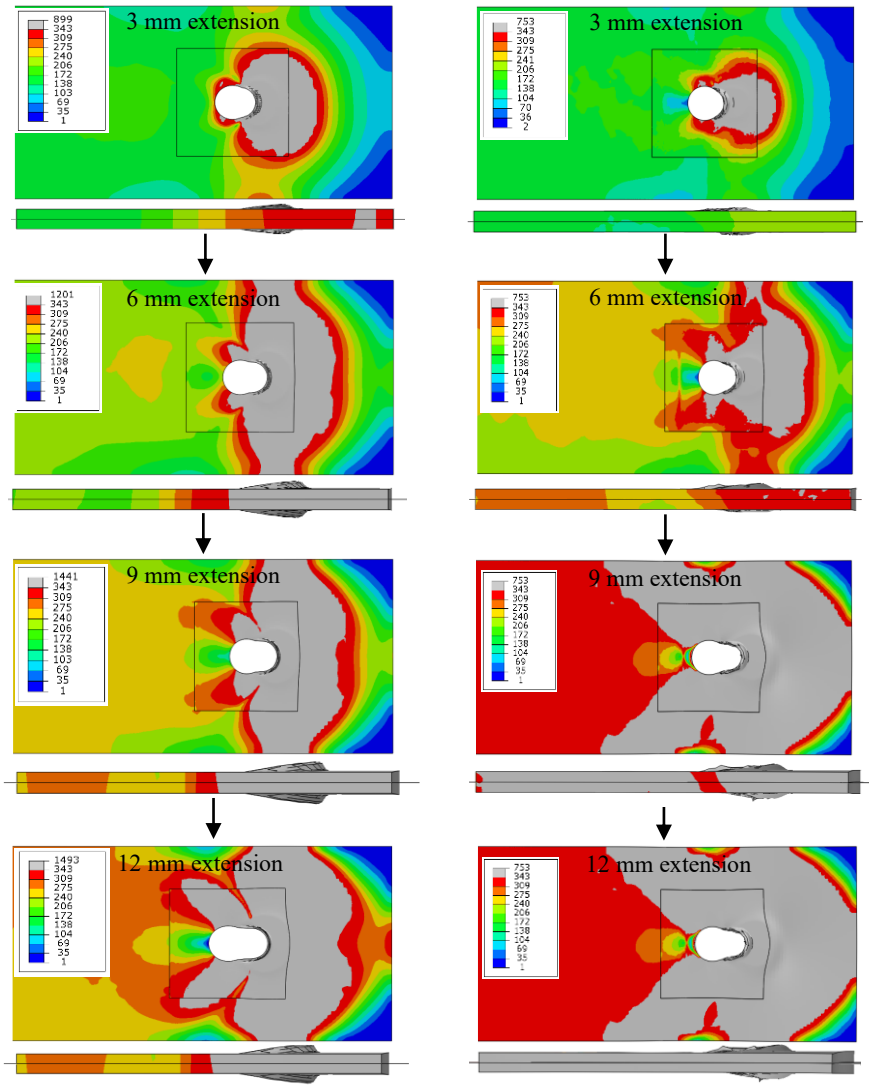

(a) Partially-threaded bolt (b) Threaded bolt

Fig. 13 Evolution of yielding with increasing displacement for specimens with partially-threaded and threaded bolts [27] (contour units: N/mm^2)

The effect of bolt pretension was also investigated for the specimens examined in [27]. Assuming a torque of 20 Nm, a preloading force of 11 kN was calculated, as described in Section 3.4, which was then applied within the bolt shank through a temperature field, resulting friction forces, shown in Fig. 14, were found to be similar to the theoretical values determined from Equation (9). The coefficient of thermal expansion of the steel was taken as 1.2×10^{-5}/°C, while the assigned temperature difference was set equal to 198°C to achieve a preloading force of 11 kN in the bolt shank. Furthermore, the predicted slippage distance of approximately 2 mm (see Fig. 14) aligns with the sum of the 1 mm distance between the bolt shank and the test plate and the 1 mm distance between the bolt shank and the hot-rolled plate reported in [27]. No clearance between the bolts and plates was reported in [37].

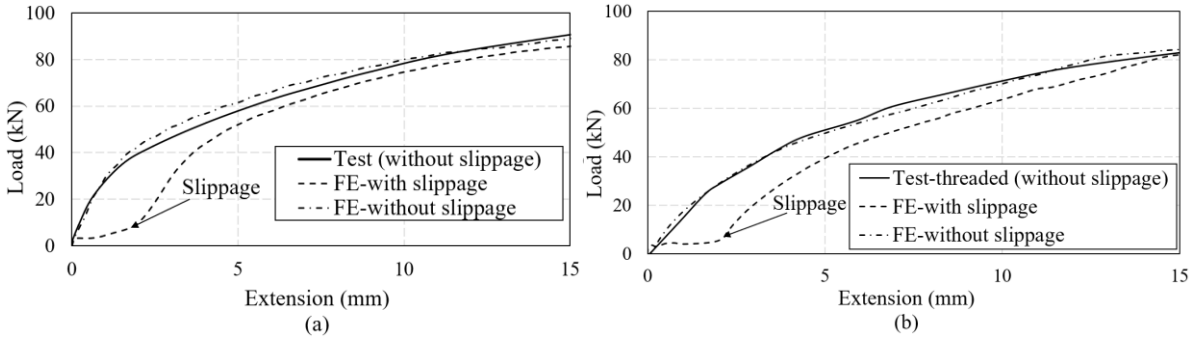

Fig. 14 Load-extension curve of lap joint considering pretension force with: (a) partially-threaded and (b) fully-threaded bolts

4.2 Built-up members

In this section, the efficiency of the proposed numerical method for modelling cold-formed steel built-up sections is assessed by comparisons against physical tests [36]. An experimental programme, complemented by numerical analyses, was undertaken in [36], in order to investigate the structural behaviour of cold-formed steel built-up beams subjected to minor axis bending. The test specimens, shown in Fig. 15, comprised two cold-formed steel channel sections connected back-to-back using M12 bolts. All specimens were simply supported at their ends and subjected to 4-point bending.

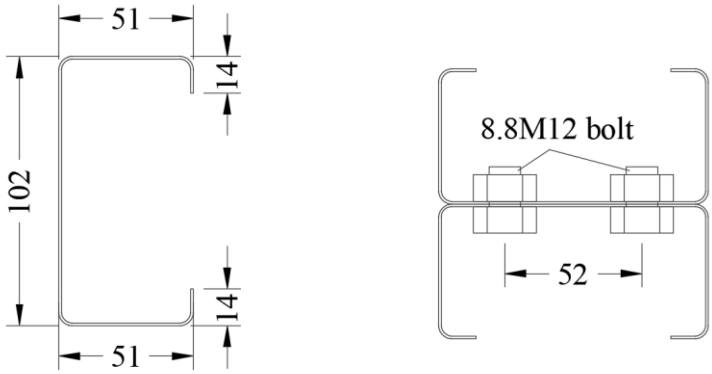

Fig. 15 Nominal dimensions (in mm) of built-up beams tested in [36]

Three specimens were selected for the validation presented herein, labelled C10010-2R-B55, C10010-4R-BF and C10010-4R-B55, all comprising C10010 cold-formed steel sections

connected back-to-back with 2 or 4 rows of bolts (labelled 2R or 4R respectively), and with the bolts being finger-tightened or installed using a torque wrench set to a torque of 55 Nm (labelled BF or B55 respectively).

The mechanical properties assigned to the modelled specimens were obtained from the material tests reported in [36]. The mesh, boundary conditions and contact pairs defined for the FE modelling of the tested built-up beams are presented in Fig.16. Replication of the boundary conditions was implemented by coupling the nodes at the beam ends to reference points, which were assigned displacement and rotation restraints as in the physical tests – see Fig. 16. Geometric imperfections were included in the numerical simulations by scaling the first positive buckling mode of the members; the magnitude of the imperfection was taken as $e = 0.2t\lambda_s$, where t is the thickness of the cold-formed steel element and λ_s is the cross-sectional slenderness [47].

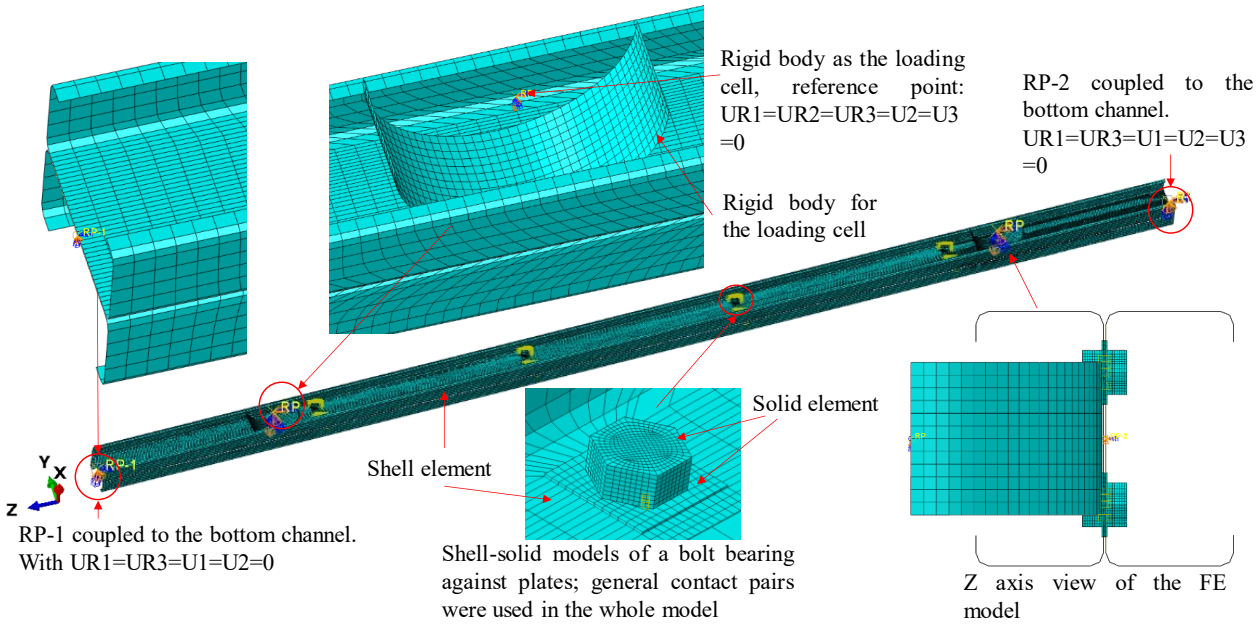

Fig. 16 FE model of specimen C10010-4R-BF

It is worth noting that, although in the study reported in [36], lap tests were also undertaken to determine the load-extension relationships of the connections, these were not employed in the FE models presented herein, since the proposed numerical method can capture the bolt-plate interaction, thus eliminating, or at least reducing, the time and cost expense of structural testing.

Three loading steps were defined in ABAQUS [39] for the FE analyses of the built-up beams: an 'Initial Step' to define the boundary conditions, a 'Prestress' dynamic explicit step to apply pretension in the bolt shanks (in line with Section 3.4) and a 'Loading Step', using a dynamic explicit displacement control scheme (in line with Section 3.3). As shown in Fig. 17, a total of 6600 s was used in the explicit FE analyses, with the target time increment set to 0.004 s.

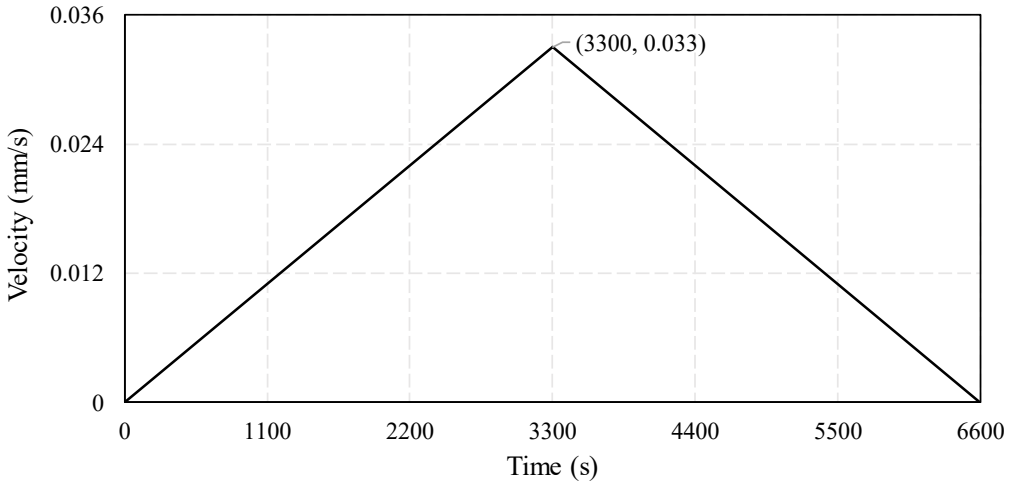

Fig. 17 Velocity-time relationship employed in the explicit FE analyses of cold-formed steel built-up members

Comparisons between the test and FE load-deflection (at the loading point) curves are shown in Fig. 18, where it can be observed that the numerical simulations provide accurate predictions of the deserved experimental behaviour, both in terms of strength and stiffness. The initial linear part of all load-deflection curves, which was very accurately captured by the FE models, reflects the flexural rigidity of the built-up beams, which was the focus of investigation presented in [36]. The multiple drops in load evident in both the test and FE load-deflection curves correspond to the sequential formation of distortional buckles along the member length.

The failure modes predicted by the FE models were also found to be in good agreement with the relevant test descriptions reported in [36]. The progression of deformation and evolution of von Mises stresses for a typical specimen are shown in Fig.19(a) to (d). In Fig.19(a) the specimen is within the initial linear portion of the load-deformation response. This is followed by distortional buckling, localised yielding and the separation of the webs of the channel sections, which were initially in contact, at a number of points along their lengths. A comparison of failure modes obtained from the test and FE model for a typical C10010 built-up specimen is shown in Figure 20, where good agreement can be observed.

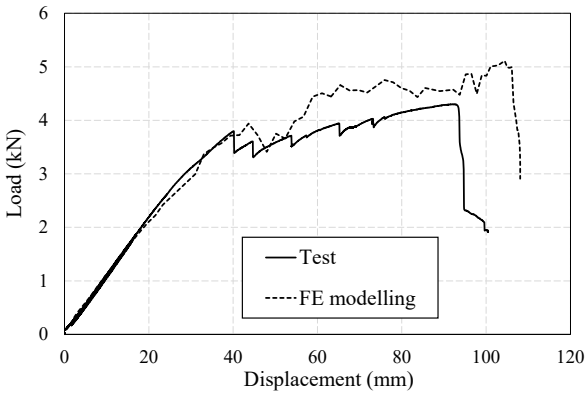

(a) Specimen C10010-2R-B55

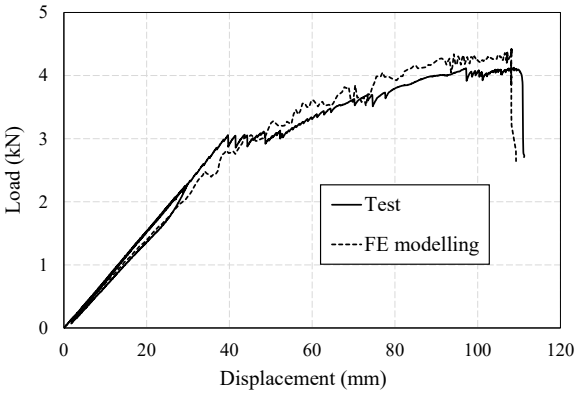

(b) Specimen C10010-4R-BF

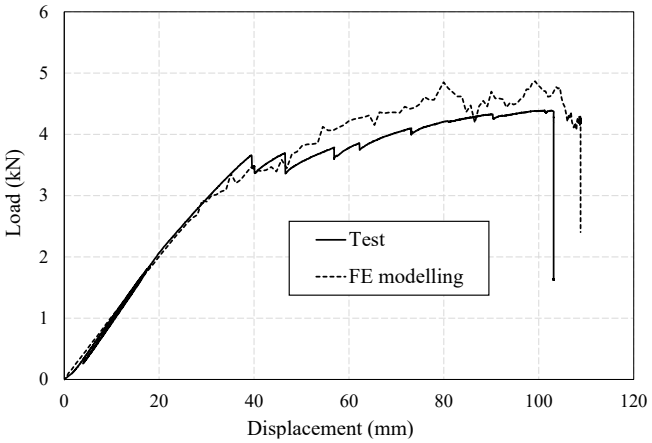

(a) Specimen C10010-4R-B55

Fig. 18 Test and FE load-deflection curves of built-up beams [36]

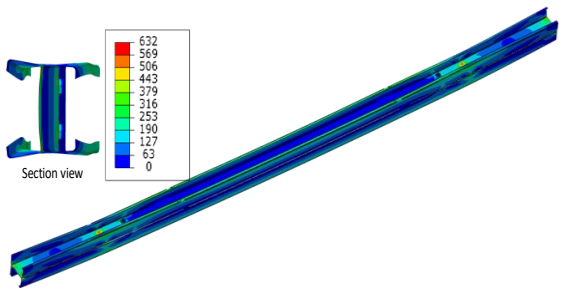

(a) Loading point: δ = 20 mm

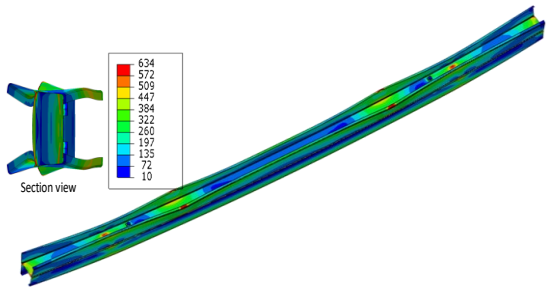

(b) Loading point: δ = 40 mm

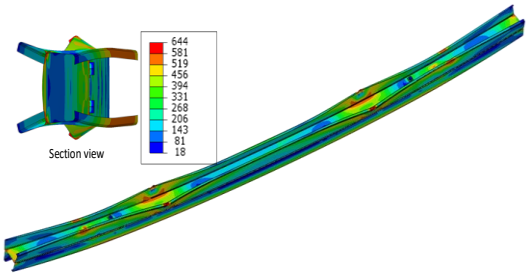

(c) Loading point: δ = 60 mm

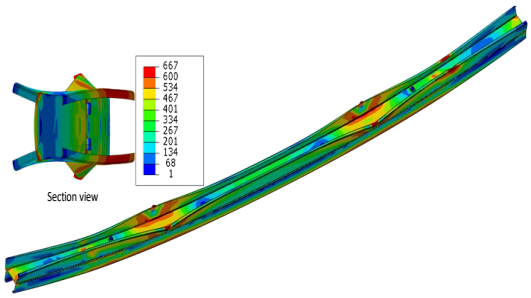

(d) Loading point: δ = 80 mm

Fig. 19 Spreading of yielding with increasing load for a typical built-up specimen (contours showing von Mises stresses in N/mm^2)

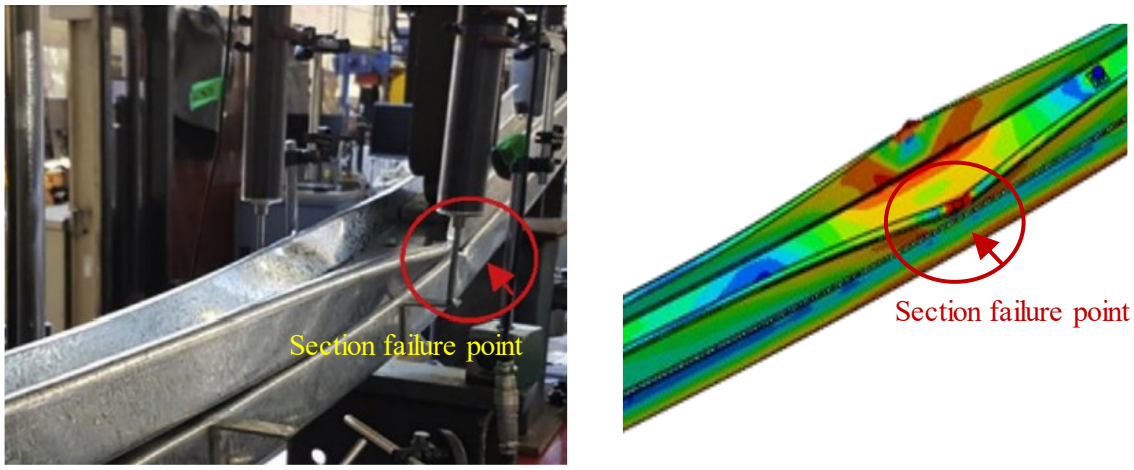

(a) Failure mode from test (b) Failure mode from FE modelling

Fig. 20 Typical failure mode of C10010 built-up specimens from: (a) test and (b) FE modelling

Slip at the interface between the two channel sections of test specimen C10010-2R-B55 was observed in the physical experiment [36], despite the two rows of bolts being preloaded through the application of a 55 Nm torque, resulting in bearing of the bolts into the surrounding material. This behaviour was also captured by the developed FE model, as shown in Fig. 21, building further confidence on the reliability of the proposed numerical method.

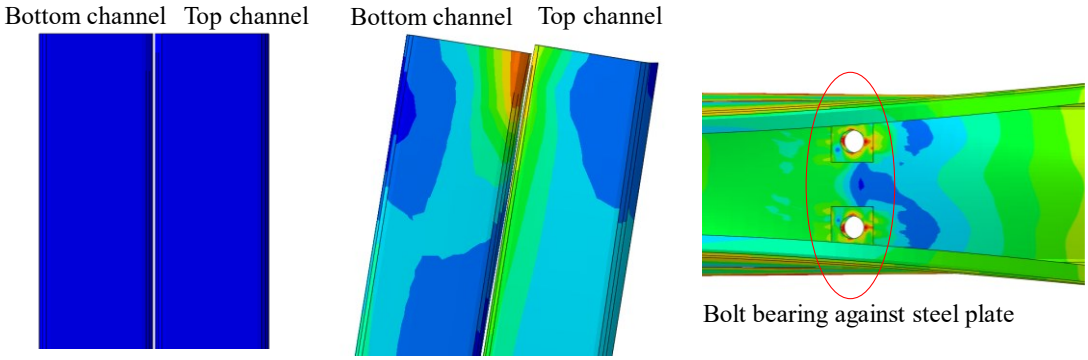

(a) δ_{mid} = 0 mm (b) δ_{mid} = 80 mm

Fig. 21 Slip at the interface between the two channel sections (specimen C10010-2R-B55)

5 Application of the proposed modelling approach

An accurate modelling technique that combines shell elements and a small number of solid elements around the bolt holes has been presented and shown to be capable of capturing the behaviour of thin-walled bolted connections and built-up members. Some recommendations on the practical application of the proposed approach are given in this section:

(1) The square/rectangular blocks created around the bolt holes should be modelled with solid elements, while shell elements should be assigned to the other modelled parts of the members. Continuity between the solid and shell elements at the interface of the blocks should be established through the application of coupling constraints.

(2) The size of the block around the bolt holes should be sufficiently large to cover the areas of major influence of the bolt nut and bolt head, thus allowing material piling up to be captured and a smooth force transition between the solid and shell elements. It is therefore recommended that the length of each side of the block is equal to $2d+10\ mm$, where d is the length of each side of the hexagonal bolt head.

(3) A sufficiently fine mesh should be employed for the blocks around the bolt holes to achieve high computational accuracy. A mesh size of up to 1/4 of the plate thickness is therefore generally recommended, but a mesh sensitivity study should be carried out to determine a suitable balance between accuracy and computational efficiency.

6 Conclusions

A practical numerical method for the simulation of bolted cold-formed steel connections has been introduced in this paper. At the core of the proposed finite element (FE) methodology is the balanced combination of shell and solid elements, with the bolt and the surrounding material being modelled with solid elements, to accurately capture the plate-fastener interaction, and the remainder of the steel plates modelled with shell elements, to ensure numerical efficiency and stability. The proposed method accounts for all the key features that influence the behaviour of connections in thin-walled steel members, including bolt preload, slippage and bearing, while the accurate replication of the bolt-ply interaction is achieved by the definition of contact pairs between the bolts and the surrounding material.

The developed FE models were validated against benchmark tests reported in the literature. It has been shown that the proposed numerical approach can accurately capture the structural behaviour of bolted cold-formed steel connections and cold-formed steel built-up sections, while being computationally efficient and numerically stable; its use is therefore recommended for the numerical simulation of cold-formed steel members assembled using fasteners.

Acknowledgements

The authors would like to thank Mr Dang K. Phan at the University of Sydney for discussions and providing experimental data for the model validation.

References

[1] AS/NZS 4600: Cold-formed Steel Structures. Standards Australia Sydney, Australia; 2018.
[2] CEN/EN Eurocode 3, Part 1-3: Design of steel structures: General rules-Supplementary rules for cold-formed members and sheeting. European Committee for Standardization, Brussels. 2006.
[3] AISI. North American specification for the design of cold-formed steel structural members: American Iron & Steel Institute, Committee of Steel Plate Producers; 2007.
[4] Winter G. Tests on bolted connections in light gage steel. Journal of the Structural Division-ASCE. 1956;82:1-25.
[5] Teh LH, Clements DD. Block shear capacity of bolted connections in cold-reduced steel sheets. Journal of Structural Engineering-ASCE. 2012;138:459-67.
[6] Teh LH, Uz ME. Effect of loading direction on the bearing capacity of cold-reduced steel sheets. Journal of Structural Engineering-ASCE. 2014;140:06014005.
[7] Teh LH, Uz ME. Ultimate Tilt-Bearing Capacity of Bolted Connections in Cold-Reduced Steel Sheets. Journal of Structural Engineering-ASCE. 2017;143:04016206.
[8] Teh LH, Gilbert BP. Net section tension capacity of bolted connections in cold-reduced steel sheets. Journal of Structural Engineering-ASCE. 2012;138:337-44.

[9] Xing H, Teh LH, Jiang Z, Ahmed A. Shear-Out Capacity of Bolted Connections in Cold-Reduced Steel Sheets. Journal of Structural Engineering-ASCE. 2020;146:04020018.
[10] Zadanfarrokh F, Bryan E. Testing and design of bolted connections in cold formed steel sections. 11th International Specialty Conference on Cold-Formed Steel Structures. Missouri University of Science and Technology1992.
[11] Winter G. Light gage steel connections with high-strength, high-torqued bolts. Missouri University of Science and Technology; 1956.
[12] Rogers C, Hancock G. Bolted connection design for sheet steels less than 1.0 mm thick. Journal of Constructional Steel Research. 1999;51:123-46.
[13] Cai Y, Young B. Carbon steel and stainless steel bolted connections undergoing unloading and re-loading processes. Journal of Constructional Steel Research. 2019;157:337-46.
[14] Cai Y, Young B. Structural behavior of cold-formed stainless steel bolted connections. Thin-Walled Structures. 2014;83:147-56.
[15] Elliott MD, Teh LH, Ahmed A. Behaviour and strength of bolted connections failing in shear. Journal of Constructional Steel Research. 2019;153:320-9.
[16] Wang Y-B, Lyu Y-F, Li G-Q, Liew JR. Behavior of single bolt bearing on high strength steel plate. Journal of Constructional Steel Research. 2017;137:19-30.
[17] Salih E, Gardner L, Nethercot D. Bearing failure in stainless steel bolted connections. Engineering structures. 2011;33:549-62.
[18] Salih E, Gardner L, Nethercot D. Numerical investigation of net section failure in stainless steel bolted connections. Journal of Constructional Steel Research. 2010;66:1455-66.
[19] Nethercot D, Salih E, Gardner L. Behaviour and design of stainless steel bolted connections. Advances in Structural Engineering. 2011;14:647-58.
[20] Ahmed A, Teh LH. Thread effects on the stiffness of bolted shear connections. Journal of Constructional Steel Research. 2019;160:77-88.
[21] Kim TS, Kuwamura H, Cho T. A parametric study on ultimate strength of single shear bolted connections with curling. Thin-Walled Structures. 2008;46:38-53.
[22] Lyu Y-F, Wang Y-B, Li G-Q, Jiang J. Numerical analysis on the ultimate bearing resistance of single-bolt connection with high strength steels. Journal of Constructional Steel Research. 2019;153:118-29.
[23] Lyu Y-F, Li G-Q, Wang Y-B, Li H, Wang Y-Z. Bearing behavior of multi-bolt high strength steel connections. Engineering Structures. 2020;212:110510.
[24] Kim TS, Kuwamura H, Kim S, Lee Y, Cho T. Investigation on ultimate strength of thin-walled steel single shear bolted connections with two bolts using finite element analysis. Thin-Walled Structures. 2009;47:1191-202.
[25] Kyvelou P, Kyprianou C, Gardner L, Nethercot D. Challenges and solutions associated with the simulation and design of cold-formed steel structural systems. Thin-Walled Structures. 2019;141:526-39.
[26] Perera D, Pologanathan K, Gillie M, Gatheeshgar P, Sherlock P, Nanayakkara S et al. Fire performance of cold, warm and hybrid LSF wall panels using numerical studies. Thin-Walled Structures. 2020;157:107109.
[27] Lim JB, Nethercot D. Stiffness prediction for bolted moment-connections between cold-formed steel members. Journal of Constructional Steel Research. 2004;60:85-107.
[28] Zaharia R, Dubina D. Stiffness of joints in bolted connected cold-formed steel trusses. Journal of Constructional Steel Research. 2006;62:240-9.
[29] Yu W, Chung K, Wong M. Analysis of bolted moment connections in cold-formed steel beam–column sub-frames. Journal of constructional steel research. 2005;61:1332-52.
[30] Kechidi S, Fratamico DC, Schafer BW, Castro JM, Bourahla N. Simulation of screw connected built-up cold-formed steel back-to-back lipped channels under axial compression. Engineering Structures. 2020;206:1101-09.
[31] Rinchen R, Rasmussen KJ. Numerical modelling of cold-formed steel single C-section portal frames. Journal of Constructional Steel Research. 2019;158:143-55.
[32] Ye J, Mojtabaei SM, Hajirasouliha I, Shepherd P, Pilakoutas K. Strength and deflection behaviour of cold-formed steel back-to-back channels. Engineering Structures. 2018;177:641-54.

[33] Ye J. More efficient cold-formed steel elements and bolted connections: University of Sheffield; 2016.
[34] Ye J, Mojtabaei SM, Hajirasouliha I. Seismic performance of cold-formed steel bolted moment connections with bolting friction-slip mechanism. Journal of Constructional Steel Research. 2019;156:122-36.
[35] Ye J, Mojtabaei SM, Hajirasouliha I, Pilakoutas K. Efficient design of cold-formed steel bolted-moment connections for earthquake resistant frames. Thin-Walled Structures. 2020;150.
[36] Phan DK, Rasmussen KJ. Flexural rigidity of cold-formed steel built-up members. Thin-Walled Structures. 2019;140:438-49.
[37] Chung K, Ip K. Finite element modeling of bolted connections between cold-formed steel strips and hot rolled steel plates under static shear loading. Engineering Structures. 2000;22:1271-84.
[38] Schafer BW, Li Z, Moen CD. Computational modeling of cold-formed steel. Thin-Walled Structures. 2010;48:752-62.
[39] Abaqus/CAE User's Manual. 2019.
[40] Ramberg W, Osgood W. Determination of stress-strain curves by three parameters. NACA Technical Note. 1941.
[41] Gardner L, Yun X. Description of stress-strain curves for cold-formed steels. Construction and Building Materials. 2018;189:527-38.
[42] Hu Y, Shen L, Nie S, Yang B, Sha W. FE simulation and experimental tests of high-strength structural bolts under tension. Journal of Constructional Steel Research. 2016;126:174-86.
[43] Yu H, Burgess I, Davison J, Plank R. Numerical simulation of bolted steel connections in fire using explicit dynamic analysis. Journal of Constructional Steel Research. 2008;64:515-25.
[44] Juvinall RC, Marshek KM. Fundamentals of machine component design: John Wiley & Sons New York; 2006.
[45] Bickford JH. An introduction to the design and analysis of bolted joints. Marcel Dekker, New York; 1997.
[46] Wong MF, Chung KF. Structural behaviour of bolted moment connections in cold-formed steel beam-column sub-frames. Journal of Constructional Steel Research. 2002;58:253-74.
[47] Dawson RG, Walker AC. Post-buckling of geometrically imperfect plates. Journal of the Structural Division-ASCE. 1972;98:75-94.